



Genetic-Algorithm-Based Optimization Approach for Energy Management

Prof. G. B. Hangaragi* and Prof. Santosh Kolaki**

*Associate professor, VSM Institute of Engineering, Nipani-591237 Belgaum

**Associate professor, VSM Institute of Engineering, Nipani-591237 Belgaum

(Corresponding Author: Prof. G. B. Hangaragi)

(Received 29 September, 2016 Accepted 25 October, 2016)

(Published by Research Trend, Website: www.researchtrend.net)

ABSTRACT: This paper proposes a new strategy to meet the controllable heating, ventilation, and air conditioning (HVAC) load with a hybrid-renewable generation and energy storage system. Historical hourly wind speed, solar irradiance, and load data are used to stochastically model the wind generation, photovoltaic generation, and load. Using fuzzy C-Means (FCM) clustering, these data are grouped into 10 clusters of days with similar data points to account for seasonal variations. In order to minimize cost and increase efficiency, we use a GA-based optimization approach together with a two-point estimate method. Minimizing the cost function guarantees minimum PV and wind generation installation as well as storage capacity selection to supply the HVAC load. Different scenarios are examined to evaluate the efficiency of the system with different percentages of load shifting. The maximum capacity of the storage system and excess energy are calculated as the most important indices for energy efficiency assessment. The cumulative distribution functions of these indices are plotted and compared. A smart-grid strategy is developed for matching renewable energy generation (solar and wind) with the HVAC load.

Key words: Energy efficiency, genetic-algorithm (GA)-based optimization approach, HVAC load, probabilistic modeling, smart grid strategy, two-point estimate method.

a, b	Shape parameters for Beta distribution	S	Maximum capacity of the storage system.
A_c	Surface area of the PV array.	St	Energy stored in the storage system at time .
c	Cluster number.	t	Time.
C	Total number of clusters	v	Wind speed.
C_p	Cost of power rating of the storage system	v_i	Cut-in wind speed.
C_{pv}	Installation cost of the storage system	v_o	Cut-out wind speed.
C_s	Installation cost of the storage system	v_r	Rated wind speed
C_w	Installation cost of wind	$x_{k,1}, x_{k,2}$	Concentrations of .
d	Hourly self-discharge rate of the storage System.	X_k	th input random variable
EE	Excess energy.	apv	Installed capacity of PV
EEt	Excess energy at hour.	aw	Installed capacity of wind
f_{x_k}	PDF for the th input random variable	δ	Percentage of HVAC load to be shifted to the next hour.
G_{pv}	Net PV output power.	η_{pv}	Efficiency of the PV power interface
G_w	Net output power of the wind generator	η_s	Roundtrip efficiency of the storage system
$G_{pv,t}$	PV power generation at hour.	η_w	Efficiency of the wind power interface
$G_{w,t}$	Wind power generation at hour.	η_{pv}	Efficiency of the PV array.
$G_{w,r}$	Wind rated power	λ	Scale parameter for Weibull distribution
G_{pv}	PV output power.	$\Lambda k, \lambda$	Coefficient of skewness for .
G_w	Output power of the wind generator	μX_k	Expected value of the th input random variable
k	Shape parameter for Weibull distribution	$\xi_{K,1}, \xi_{K,2}$	Locations of concentrations.
L_t	Load demand at hour.	X_K	standard deviation of the th input random Variable.
L_t	Modified HVAC loads at hour.	T	Gamma function.
$L_{s,t}$	Shifted load demand at time		
P	Maximum power rating of the storage system.		
$P_{k,1}, P_{k,2}$	Probabilities of concentrations		
P_t	Power rating of the storage system at time .		

I. INTRODUCTION

The world is currently increasing its use of renewable energy and decreasing its reliance on imported fossil fuels. The development of the smart grid will facilitate the integration of renewable energy sources into the power grid. Smart-grid applications include transmission, distribution, and distributed generation [1]. The “smarter” monitoring and control will create a more efficient energy-management system for residential customers. Smart-grid applications in distribution systems include smart metering technologies for efficient integration of distributed renewable generation applications, fair pricing mechanisms, remote monitoring, and home automation and control of electrical power consumption. However, the stochastic nature of PV and wind energy resources complicates the integration of renewable generation applications. In addition, wind is often not correlated with the load pattern and may be discarded even when abundantly available [2], [3]. The U.S. Department of Energy estimates that HVAC loads account for 40%–60% of the energy consumption in U.S. commercial and residential buildings [4]. Since these time-flexible loads are deferrable for a few minutes or hours at little or no cost, their energy consumption can be adapted according to the renewable power-supply fluctuation. This demand-side flexibility can counterbalance renewable supply variations and efficiently integrate renewable generation. Energy efficiency can be further increased by storing energy when renewable power generation exceeds the load requirements then releasing it when renewable generation is insufficient to supply the load [5]. The efficiency of a hybrid system is dependent on the renewable generation efficiency, the self-discharge rates, and roundtrip efficiencies of the energy storage units, and on the sizing of the system components [6], [7]. The design, simulation, and optimization of hybrid power systems have been the subjects of several studies [8]–[18]. Operating concepts, performance evaluation, and economic analysis of such systems were investigated in [8]–[12] where the component sizing is either arbitrary or based on practical and experimental estimates, with no attempt at optimizing their parameter values. References [13]–[17] employed a variety of heuristic optimization techniques for the optimal design and operation of the hybrid systems. However, none of these investigations focused on demand flexibility and HVAC loads, in particular, or on matching HVAC loads with renewable energy sources without the need for supplementary conventional generations. Reference [18]

presented an optimal component-sizing framework for the hybrid system, but the stochastic nature of wind/PV generation is not considered in the modeling. Emerging smart-grid strategies can provide the distribution system with an opportunity to balance renewable generation and HVAC loads for a residential feeder using energy storage systems. A smart load shifting strategy is proposed in this paper to shift the HVAC loads based on parameters which characterize the load flexibility, such as the percentage of load to be shifted, or the deadline by which this load should be met. Unlike [13]–[17], which utilized conventional generation to complement a hybrid system, the proposed strategy eliminates the need for supplementary generation and meets the HVAC load at the desired confidence level. The proposed approach uses FCM to obtain data clusters for characterizing seasonal variations. This provides a better representation of the system's behavior than earlier work [8]–[18]. In addition, the proposed methodology characterizes the uncertainties of the stochastic variables (wind speed, solar irradiance, and HVAC load) which are not addressed in [18]. The combination of the GA and two-point estimation enhances the efficiency of the hybrid system when compared to classical optimization approaches. This paper proposes a smart-grid strategy for matching renewable energy generation with HVAC loads using hybrid renewable energy generation and energy storage. Section III explains the new GA optimization and two-point estimation methodology, reviews FCM clustering, and explains how it is used to cluster historical hourly wind speed/clearness index/load data. It also presents stochastic models of wind and PV generation and HVAC load based on actual data. Different scenarios are studied and their simulation results are given in Section IV. Conclusions are presented in Section V.

II. METHODOLOGY

A. Probabilistic Modeling of Generation and HVAC Load Hybrid generation systems are inherently uncertain because of the stochastic nature of wind speed, solar irradiance, and load characteristics. The uncertainties of wind/solar generation are characterized using the probability density functions (PDFs) whose statistics are obtained from historical data of wind speed and solar irradiance [19], [20]. FCM clustering is used in this paper to account for seasonal variation in the data [21].

Ten years of historical hourly data are utilized to produce three datasets for: wind speed, solar irradiance, and load [22]. Each datapoint is specified by a membership grade between 0 and 1. The objective function of the FCM is to minimize the distance from any given data point to a cluster center weighted by that datapoint's membership grade. An iterative algorithm is used to update the cluster centers and the membership grades for each datapoint, which moves the cluster centers to the most appropriate location within the data sets. The elbow method is used to determine the number of clusters [23]. Accordingly, the days are grouped into 10 clusters with similar 24-h wind speed, solar irradiance and load data. Maximum-likelihood estimates of the distribution parameters are calculated for the historical hourly data within a cluster. Each cluster is then represented by three sets of 24 individual PDFs over the 24-h period.

a) Hourly Wind Power Modeling: Wind speed is statistically modeled using the Weibull distribution [19], [20]. The PDF for a Weibull distribution is given by

$$f_v(v) = \left(\frac{k}{\lambda}\right) \left(\frac{v}{\lambda}\right)^{k-1} e^{-\left(\frac{v}{\lambda}\right)^k}, \quad 0 \leq v \leq \infty. \quad (1)$$

Using curve fitting, maximum-likelihood estimates of the Weibull distribution parameters are calculated for historical hourly wind speed data. The output power of a wind generator is a function of wind speed and given by [24]:

$$G'_W = \begin{cases} 0 & v \leq v_i, v \geq v_o \\ \frac{v - v_i}{v_r - v_i} G_{Wr} & v_i \leq v \leq v_r \\ G_{W-} & v_r \leq v \leq v_o. \end{cases} \quad (2)$$

If the power-electronic interface has an efficiency of η_w the net wind power output is given by

$$G_w = \eta_w \cdot G'_W. \quad (3)$$

b) Hourly Photovoltaic Power Modeling: Unlike wind speed, the uncertainty of solar irradiance cannot be directly modeled using a PDF. This is due to the fact that the solar irradiance has very strong diurnal patterns as at night time; the value of solar irradiance

is certain to be zero [25]. Hence, this paper uses the clearness index (k_t) to characterize solar irradiance. The hourly clearness index is defined as the ratio of the irradiance on a horizontal plane I_t (kW/m^2), to the extraterrestrial total solar irradiance I_o (kW/m^2)

$$k_t = \frac{I_t}{I_o}. \quad (4)$$

The clearness index is statistically modeled using the beta distribution [20], [26]. The PDF for a beta distribution over a time interval t is given by

$$f_{ci}(k_t) = \frac{\Gamma(a+b)}{\Gamma(a)\Gamma(b)} \cdot k_t^{a-1} \cdot (1-k_t)^{b-1}. \quad (5)$$

Using curve-fitting, maximum-likelihood estimates of the beta distribution parameters are calculated for historical hourly clearness index data. Once the hourly clearness index is known, the irradiance on a surface with inclination β to the horizontal plane is I_β calculated as

$$I_\beta = T \cdot k_t - T' \cdot k_t^2 \quad (6)$$

where T and T' are parameters that depend on inclination, declination, reflectance of the ground, latitude, hour angle, and sun set hour angle. The PV power output is a function of the clearness index and is given by [19]

$$G'_{PV} = A_c \cdot \eta'_{PV} \cdot I_\beta = A_c \cdot \eta'_{PV} \cdot (T \cdot k_t - T' \cdot k_t^2). \quad (7)$$

If the power-electronic interface has an efficiency of η_{pv} then the PV power output is given by

$$G_{PV} = \eta_{PV} \cdot G'_{PV}. \quad (8)$$

The values for T and T' are calculated using the efficiency curves of the power converters [27], [28].

c) Hourly Load Modeling: This paper uses a Gaussian distribution with specific lower and upper limits to model the hourly load variation [20]. Using curve fitting, maximum-likelihood estimates of its parameters are calculated for historical hourly load data.

B. Optimization Approach Based on the GA Method

Optimization using GAs provides a powerful tool to obtain the optimal capacity for solar energy, wind energy, and storage in a hybrid system. Generally, a set of initial solutions (initial populations), randomly selected from the feasible solution space, is used to start the GA. The fitness function is evaluated for each solution, and the solutions are consequently ranked.

The population then evolves through several operations, such as reproduction, crossover, and mutation to optimize the fitness function and obtain the final optimal solution. The process is repeated until a termination criterion is satisfied. This evolutionary algorithm is preferred to classical optimization approaches because it can handle the nonlinear, nonconvex, and nonsmooth optimization problem of the component sizing for the hybrid system. The nonconvexity of the problem makes it difficult for classical optimization methods to obtain a global optimum. GAs, on the other hand, globally search the domain of possible solutions for an optimal solution [29]–[31].

Several implementation provisions are considered in this paper to avoid convergence to local minima. In this regard, the double vector representation rather than the binary one is used for chromosome codification to guarantee mutation coherence. Scaling the decision variables and using megawatts/megawatt-hours (MW/MWh), instead of kilowatts/kilowatt-hours (kW/kWh) for the components sizing keeps the feasible solution space smaller and facilitates mutation.

A large population size is selected to increase the possibility of convergence to the global minimum, but this significantly increases the computational burden. Two elitism children are maintained for each generation to ensure retaining desirable solutions. The balance between crossover and mutation offspring is kept at a desirable level by adjusting the crossover rate around 78%.

To ensure satisfying the constraints, a large penalty factor is assigned to a solution that violates a constraint. Enhanced system efficiency as well as the fewer number of variables provided by the GA make it a better solution than classical optimization approaches for optimal component sizing of hybrid systems. The parameters of the GA are given in Table III. Using historical hourly data for wind and PV generation and cooling load, we first normalize the PV and wind generation curves by dividing them by the maximum PV and wind generation.

Next, we assign the scaling parameters α_{PV} and α_W to the normalized PV and wind curves which show the installed capacities of PV and wind generation. We obtain the optimum scaling parameters α_{PV} and α_W as well as the storage capacity by minimizing the cost function

$$\text{Min Cost} = \text{Min}\{C_{PV} \cdot \alpha_{PV} + C_W \cdot \alpha_W + C_S \cdot S + C_P \cdot P\}. \quad (9)$$

The last two terms are the capital costs needed for installing the storage system. The total capital cost of the storage system is composed of four components: 1) the capital cost for energy; 2) the capital cost for power; 3) the system energy balance cost; and 4) the system power balance cost. The balance of system energy and power cost can be included in C_S and C_P , respectively [32]. Also, the inverter-based interface cost for connecting the PV and wind to the network is considered part of C_{PV} and C_W . The optimization formula given in (9) is subject to several physical constraints on the parameters. The first constraint is an energy balance equation to guarantee that the combination of wind and PV generation meets the required HV or cooling load over the optimization period. Note that the efficiency of the storage system is always less than unity due to the losses. To compensate for these losses, additional generation is needed. Hence, the energy balance equation must be changed to the following inequality constraint:

$$\sum_{t=1}^T G_{PV,t} + \sum_{t=1}^T G_{W,t} \geq \sum_{t=1}^T L_t \quad (10a)$$

$$E = \sum_{t=1}^T E_t = \sum_{t=1}^T G_{PV,t} + \sum_{t=1}^T G_{W,t} - \sum_{t=1}^T L_t. \quad (10b)$$

The next constraint guarantees an instantaneous balance between the sum of the generated wind energy, PV energy, and stored energy, and the instantaneous load. The storage is charged

When $G_{PV,t} + G_{W,t} - L_t + L_{S,t} \geq 0$ and discharged when $G_{PV,t} + G_{W,t} - L_t + L_{S,t} < 0$. The instantaneous energy balance in the storage system is as follows:

a) For charging

$$S_t = (1 - d)S_{t-1} + \eta_S(G_{PV,t} + G_{W,t} - L_t + L_{S,t}) \quad \forall t \in T. \quad (11a)$$

b) For discharging

$$S_t = (1 - d)S_{t-1} + (G_{PV,t} + G_{W,t} - L_t + L_{S,t}) \quad \forall t \in T. \quad (11b)$$

Utilities often have some intelligent control over HVAC loads, including agreements with consumers to shift part of their HVAC loads during peak load hours, if there is a problem in the operation of the transmission network. For example, NV Energy's cool share program is associated with an approximate 145-MW remote-controlled air conditioning load. These loads can be dispatched by NV Energy through "raise/lower" thermostat commands as needed and may include pool pumps, refrigerators, hot tubes, etc. which "need to run" but their exact time of operation is not critical. Load shifting can provide some flexibility regarding this problem. Since the hourly generation of wind farms and solar plants is not strictly under human control, load shifting can be useful during periods of insufficient generation. Implementing smart load control can reduce the mismatch between renewable generation and HVAC load. Load shifting is expressed as

$$L'_t = L_t - L_{S,t} \quad (12a)$$

$$L'_{t+1} = L_{t+1} + L_{S,t}. \quad (12b)$$

To ensure that the shifted load is positive and is less than the specific percentage of the load at each time, we need

$$0 \leq L_{S,t} \leq \delta \cdot L_t. \quad (13)$$

Storage systems have a minimum storage level, denoted by, that must be maintained to prolong lifetime. In addition, there is typically a maximum storage capacity that is dictated by the size of the renewable generation units, which we denote as. The storage at time is thus governed by

$$S_{\min} \leq S_t \leq S_{\max}. \quad (14)$$

The upper bound is not known *a priori* and is optimally calculated in our solution. The next constraint ensures that the capacity of the storage system is equal to the maximum storage capacity needed to maintain excess energy at hour

$$S = \max(S_t), \quad (15)$$

Assuming the same charge and discharge rate, the maximum power rating of the storage unit is given by

$$P_t = G_{PV,t} + G_{W,t} - L_t + L_{S,t} \quad (16a)$$

$$P = \max |P_t|. \quad (16b)$$

The optimization problem can be formulated as follows:

$$\min \{f(x, u)\} \quad (17)$$

$$\text{s.t. } g(x, u) = 0 \quad (18)$$

$$h(x, u) \leq 0 \quad (19)$$

where $f(x, u)$ is the objective function of (9); the decision variables are (u) are α_{PV} , α_W ; and the dependent variables (x) are EE ,

$L'_t, L'_{t+1}, S_t, S, P_t, P$. The equality constraints of (18) are given by (10b), (11a), (11b), (12), (15), and (16), while the inequality constraints of (19) are given by (13) and (14). We first solve a simplified optimal component-sizing problem without load shifting for the hybrid system using a GA implemented in MATLAB. We then solve the same problem using discontinuous nonlinear programming (DNLP) in GAMS. Table IV shows the simulation results for this problem. Comparing the GA-based results with the DNLP demonstrates the improved efficiency of the proposed methodology over the classical optimization approaches.

C. Probabilistic Optimization

The randomness of wind and PV power output and loads are taken into account by using stochastic optimization. The latter is performed using analytical methods or simulation methods [33]. Monte-Carlo simulation (MCS) is a simple and accurate simulation method that uses historical data to determine their PDFs. Random values from these PDFs are used to quantify the uncertainties. The large computational effort is the main obstacle for efficient use of this method. Several approximate methods have been proposed to reduce the computational burden including Taylor series expansion [34], first-order second-moment method (FOSMM) [35], cumulants [36], and point estimation (PE) [37]. PE is a popular analytical method because of its accuracy, simplicity, and speed. Two-point estimation (2PE), a variation of PE, is applied in this paper to model the uncertainties [38], [39]. Vectors of input and output random variables and the corresponding nonlinear function are given by (20)–(22).

$$X = [\text{Wind Gen.}, \text{PV Gen.}, \text{HVAC Load}] \quad (20)$$

$$Y = [S_t, P_t, EE_t, L_{S,t}] \quad (21)$$

$$Y = h(X). \quad (22)$$

Two concentrations $f_{x_i}(X_{k,1}, X_{k,2})$ of are used to replace f_{x_i} by matching its first three moments. The functional relation between X_k and $h(X_k)$ is then used to produce two estimates of variants

$(Y_k, l = h(\mu_{x_1}, \mu_{x_2}, \dots, x_{k,1}, \mu_{x_{n-1}}, \mu_{x_n}) | i = 1, 2)$ from $(x_{k,1}, x_{k,2})$. $P_{k,1}$ and $P_{k,2}$ scale these estimates to compute the expected value and standard deviation of the output. Fig. 1 shows the flowchart for the proposed method. Ten years of historical hourly wind speed, solar irradiance, and load data are the inputs. FCM is then used to cluster these data into clusters of days with similar data points. Next, the scaling parameters (and) are initialized. The parameters of the 2PE shown in Fig. 1 are

$$\zeta_{k,i} = \sqrt{n + \left(\frac{\lambda_{k,3}}{2}\right)^2} \quad i = 1, 2 \quad (23a)$$

$$\xi_{k,i} = \frac{\lambda_{k,3}}{2} + (-1)^{3-i} \zeta_{k,i} \quad i = 1, 2 \quad (23b)$$

$$P_{k,i} = \frac{(-1)^i \zeta_{k,i}}{2n \times \zeta_{k,i}} \quad i = 1, 2 \quad (23c)$$

$$x_{k,i} = \mu_{X_k} + \xi_{k,i} \sigma_{X_k} \quad i = 1, 2. \quad (24)$$

Once the 2PE parameters are calculated for the input random variables, (2), (3), (7), and (8) are used to calculate these parameters for the normalized net wind and PV power outputs. The

normalized outputs are then multiplied by the scaling parameters to calculate the hourly net PV and wind generation using vector Z . Note that μ_{x_i} in Z is replaced by $x_{k,i}$ ($i=1,2$), at each iteration. The power rating of the storage system at time t (P_t) is then calculated by the energy-management function (EMF). P_t If is positive, more generation is provided, and the storage system is charged. If negative, the load exceeds generation, and the storage system is discharged to supply the excess load. If the energy stored is less than S min, part of the load is shifted to the next hour. If the energy stored is less than after the maximum-allowable load shifting (a specific percentage of the HVAC load (δ)), new scaling parameters are selected by GA to satisfy this constraint. The first and second moments of the output variables are then calculated by

$$E(Y) \cong \sum_{k=1}^n \sum_{i=1}^2 (P_{k,i} \times h([\mu_{X_1}, \dots, x_{k,i}, \dots, \mu_{X_n}])) \quad (25a)$$

$$E(Y^2) \cong \sum_{k=1}^n \sum_{i=1}^2 (P_{k,i} \times h^2([\mu_{X_1}, \dots, x_{k,i}, \dots, \mu_{X_n}])). \quad (25b)$$

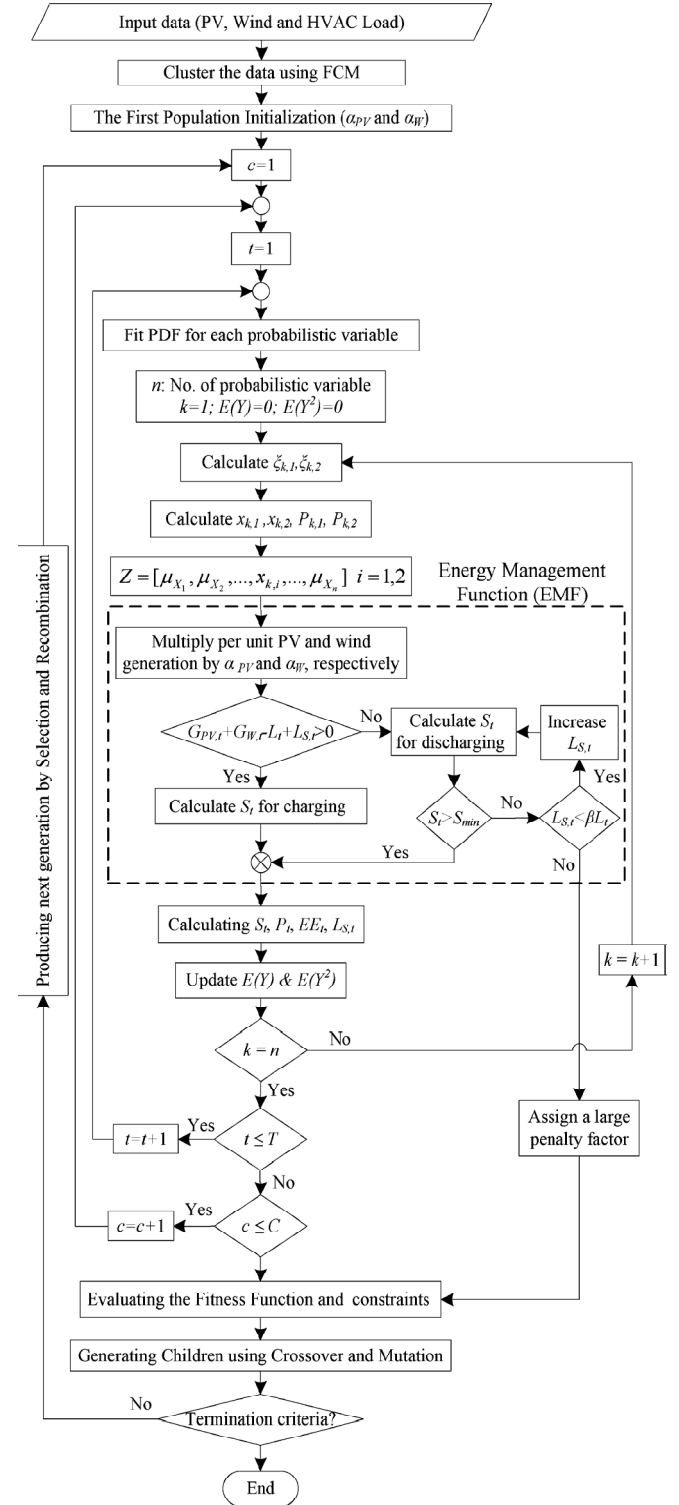
Given $E(Y)$ and $E(Y^2)$, we calculate the mean and standard deviation of the output variables

$$\mu_Y = E(Y) \quad (26a)$$

$$\sigma_Y = \sqrt{E(Y^2) - \mu_Y^2}. \quad (26b)$$

The fitness function is then evaluated, and a confidence coefficient is allocated to the probabilistic constraints

$$P(X \geq X_{\min}) \geq \gamma. \quad (27)$$



Next, the constraints are checked for violation. If there is any violation, the violated constraints are assigned a large penalty factor and combined with the fitness function to give

$$f'(x, u) = f(x, u) + \nu[h(x, u)]^2. \quad (28)$$

This combination assigns higher cost to an infeasible solution candidate than to a feasible one with the same objective values. Implementing the crossover and mutation operators to the chromosomes, the offspring population is created and then used to produce the next generation by selection and reproduction. This evolutionary algorithm is repeated until reaching the termination criterion. Eventually, the best chromosome is selected as the optimal solution. The fitness function of the GA is a weighted sum of the hybrid system installation costs for all of the clusters and is given by Fitness Function Cost (29)

$$\text{Fitness Function} = \text{Min} \left\{ \sum_{c=1}^C w_c \cdot \text{Cost}_c \right\}. \quad (29)$$

The weighting coefficient for each cluster is defined as the ratio of the number of days within that cluster to the total number of days (365/10 days). Minimizing the installation cost of the

III. CASE STUDIES

In this section, we examine two scenarios for an energy-management system combining renewable energy generation and energy storage. The first is a simplified deterministic scenario that allows us to better demonstrate the interplay between storage and renewable energy generation to meet an HVAC load. The second scenario is stochastic and includes the complexity introduced by the uncertainties of renewable energy generation and cooling loads. We present simulation results for the optimal GA or GA-2PE solution subject to the constraints (10.b) and (11)–(16).

A. Scenario I: Deterministic Wind/PV Generation and Cooling Load

Scenario I corresponds to deterministic wind generation, PV generation, and cooling load for a residential feeder over a single day [40]–[42]. The peak wind generation level is typically significantly less than the generation capacity as observed in this data set [40]. Two different cases are studied using GA-based optimization. Fig. 2 shows the hourly generation of the PV system and wind system normalized based on the maximum-installed capacities of PV and wind generation for a single day. Fig. 3 shows the hourly cooling load for a residential feeder. Installation costs of the storage system for energy and power are U.S.\$0.2/Wh, and U.S.\$0.25/W [32]. Piecewise linear cost single day functions are assigned to the PV and wind generation to calculate the associated installation costs [43], [44]. These are the average installation costs of the different technologies for utility scale (hundreds to thousands of kilowatts) systems.

The minimum-allowable charge of the storage system is 3% of its rated capacity [45]. This minimum charge, necessary for some storage technologies, is for ensuring a longer lifetime.

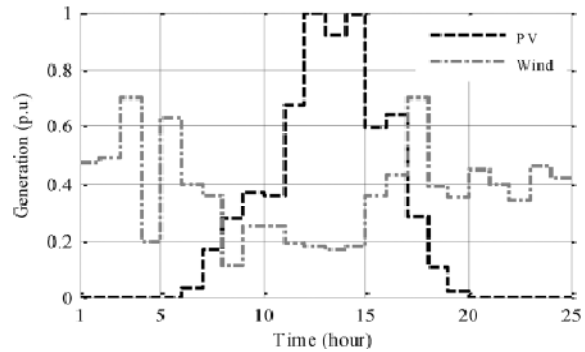


Fig. 2. Normalized hourly PV generation and wind generation.

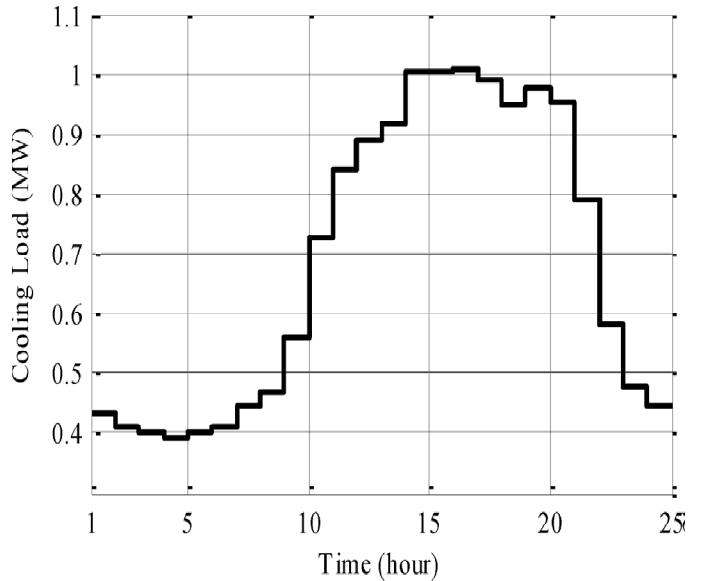


Fig. 3. Hourly cooling load of a residential feeder for a single day

Case Study I: The optimization problem is solved for the normalized PV generation, wind power, and cooling load as shown in Figs. 2 and 3. The maximum-allowable load shifting is 30% of the load for each hour. The simulation results in Fig. 4 show that in the absence of load shifting, the modified cooling load is the same as the cooling load during hours 1–15. Storage shows the state of charge of the storage system at each hour. At each hour, the energy stored in the storage system at time can be calculated by adding two components; the energy stored in the storage system at time reduced to account for discharge over one hour, and the excess energy given by the difference functions are assigned to the PV and wind generation to calculate the associated installation costs [43], [44].

These are the average installation costs of the different technologies for utility scale (hundreds to thousands of kilowatts) systems. The minimum-allowable charge of the storage system is 3% of its rated capacity [45]. This minimum charge, necessary for some storage technologies, is for ensuring a longer lifetime. *Case Study I:* The optimization problem is solved for the normalized PV generation, wind power, and cooling load as shown in Figs. 2 and 3. The maximum-allowable load shifting is 30% of the load for each hour. The simulation results in Fig. 4 show that in the absence of load shifting, the modified cooling load is the same as the cooling load during hours 1–15. Storage shows the state of charge of the storage system at each hour. At each hour, the energy stored in the storage system at time can be calculated by adding two components; the energy stored in the storage system at time reduced to account for discharge over one hour, and the excess energy given by the difference between the generation and load over a 1-h period scaled to account for the roundtrip efficiency of the storage system. As shown, wind generation is always included in the optimal solution since wind installation cost per megawatt is less than PV installation cost. The storage system is charged in the early hours of the day when more energy is available and the load is low,

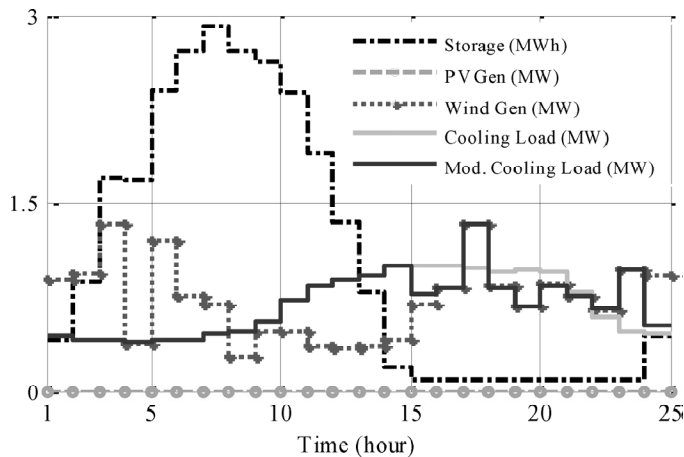


Fig. 4. Simulation result for Case Study I (Scenario I).

then releases the energy stored when the load exceeds generation. During peak hours when the wind is low and the storage is not sufficiently charged, load shifting dispatches the flexible loads to hours when the wind energy is in excess of the load. This is evident for hours 17, 22, 23, and 24 where the shifted loads are fully met. For this case study, the optimum PV, wind installation, and storage capacity are 0.0, 1.9, and 2.92 MWh (with 0.93 MW). The excess energy (i.e., the amount of energy in excess of the load) is 0.85 MWh. Total installation cost of the system is 4.615 $\times 10^6$ (3.80×10^6 for wind and 0.815×10^6 for storage).

Case Study II: This case study evaluates the possibility of matching HVAC load and PV plants, which is particularly important for regions with poor wind speed profiles and an abundance of solar energy.

The 24-h simulation period starts at noon when solar energy is most readily available. The optimum PV and storage capacity are 2.85 MW and 6.4 MWh (with 1.81 MW), and the excess energy produced is 4.58 MWh. Total installation cost of the system is minimized at 13.404×10^6 (10×10^6 for PV 1.733×10^6 for storage). The simulation results show that by installing more PV capacity and storage capacity, the load can be fully supplied without wind energy generation. Another observation is that the storage capacity needed for this case study is larger than Case Study I where wind energy is available during most hours of the day. This is because solar energy is only available during daylight hours and storage provides energy for the remainder of the day.

B. Scenario II: Stochastic Wind/PV Generation and Cooling Load

Scenario II corresponds to stochastic models of wind generation, PV generation, and cooling load. PDFs are obtained from historical hourly wind speed and solar irradiance using curve fitting [22]. Wind and PV power are derived based on (1)–(5).

Similarly, we calculate the maximum-likelihood estimates of the normal distribution parameters for historical hourly cooling load data for a residential feeder. GA-2PE stochastic optimization evaluates the efficiency of the hybrid system for 10%, 20%, 30%, 40%, and 50% load shifting (LS).

Case Study I: The GA-based optimization problem is solved considering the probabilistic PV generation, wind generation, and cooling load. Figs. 5 and 6 show the cumulative distribution functions of the storage capacity and of the excess energy (EE) for each LS. For EE, the cumulative probabilities increase with load shifting. Thus, increasing the load shifting from 10%–50% provides the system with more flexibility and reduces the storage capacity and excess energy of the system. This leads to a more efficient system with less energy dissipated due to the nonideal characteristics of the storage system.

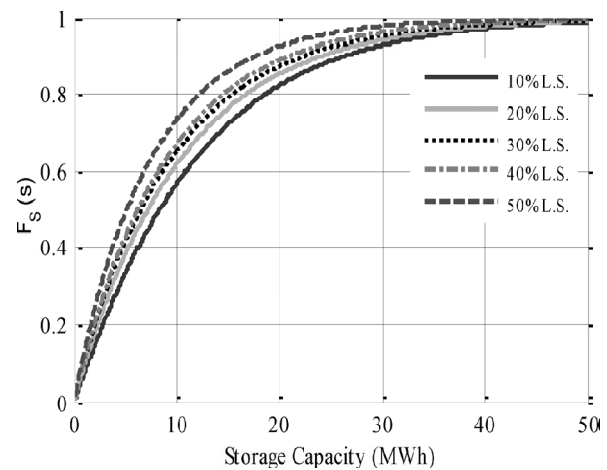


Fig. 5. Cumulative distribution of the maximum capacity of the storage system for different LS percentages (Scenario II, Case Study I).

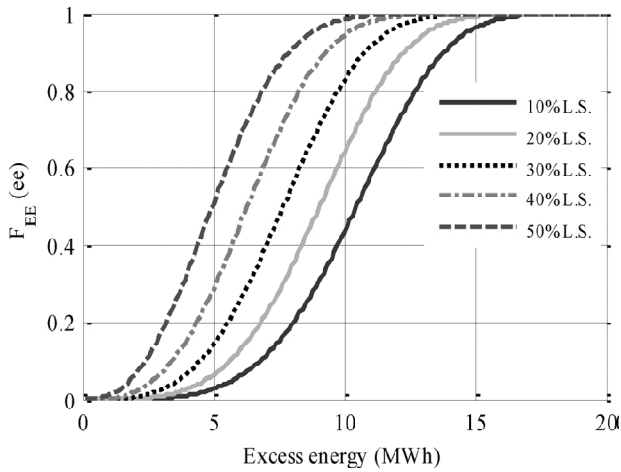


Fig. 6. Cumulative distribution of the excess energy of the system for different LS percentages (Scenario II, Case Study D).

Case Study II: This case study evaluates the possibility of matching HVAC load and PV plants for regions with poor wind speed profiles and an abundance of solar energy. The CDFs, of the storage capacity and of the excess energy (EE) for this case study show a similar trend to those of Case Study I and are not provided for brevity. For both S and EE, the cumulative probabilities increase with LS. Thus, increasing the LS from 10 to 50% provides the system with more flexibility. Table I gives the installed wind and PV capacity, the expected value, and standard deviation of storage capacity and excess energy. This table also provides optimal installation cost of the

Table 1: Installed Wind and Pv Capacity, Maximum Storage Capacity, and Excess Energy (Scenario II).

Load Shifting	10%	20%	30%	40%	50%	
Case Study I	$\alpha_w(MW)$	2.611	2.478	2.347	2.219	2.096
	$\mu_s(MWh)$	11.630	10.309	9.004	7.735	6.576
	$\sigma_s(MWh)$	11.139	10.505	9.891	9.168	7.820
	$\mu_{EE}(MWh)$	10.364	9.000	7.655	6.340	5.068
	$\sigma_{EE}(MWh)$	2.712	2.563	2.421	2.255	2.110
	Wind Cost (M\$)	5.222	4.956	4.695	4.439	4.191
	Storage Cost (M\$)	2.510	2.232	1.955	1.685	1.441
Case Study II	$\alpha_{pv}(MW)$	3.883	3.844	3.776	3.690	3.542
	$\mu_s(MWh)$	9.114	8.968	8.728	8.429	7.919
	$\sigma_s(MWh)$	4.251	4.208	3.488	3.409	3.274
	$\mu_{EE}(MWh)$	9.131	8.871	8.426	7.855	6.880
	$\sigma_{EE}(MWh)$	2.613	2.799	2.821	2.773	2.801
	PV Cost (M\$)	15.922	15.760	15.483	15.128	14.522
	Storage Cost (M\$)	2.467	2.429	2.366	2.286	2.151

Table 1 gives the installed wind and PV capacity, the expected value, and standard deviation of storage capacity and excess energy. This table also provides optimal installation cost of the hybrid system for renewable energy generation and storage systems

Table 2: Hybrid System Cost For Different Risk Levels (Scenario II).

Risk Level (%)		75	80	85	90	95
Case Study I	Wind Cost (M\$)	3.769	4.191	4.799	6.121	9.279
	Storage Cost (M\$)	1.059	1.441	2.070	3.471	6.835
Case Study II	PV Cost (M\$)	14.341	14.522	15.256	17.265	18.626
	Storage Cost (M\$)	2.111	2.151	2.315	2.782	3.102

Table II gives the cost of the hybrid system for different risk levels. Assigning a confidence coefficient to the probabilistic constraints, risk is defined as the percentage of the random variable violating the corresponding constraint

$$\text{Risk \%} = 1 - \gamma \tag{30}$$

As shown in Table I, increasing LS from 10 to 50% decreases the expected value of from 11.630 to 6.576 MWh and decreases the expected value of EE from 10.364 to 5.068 MWh for Case Study I. The same trend is observed for Case Study II, where the expected value of decreases from 9.114 to 7.919 MWh and the expected value of EE decreases from 9.131 to 6.880 MWh as LS changes from 10% to 50%. Note that renewable energy sources have already been installed in many electric utility systems across the U.S. Therefore, the total cost of the hybrid system will be significantly reduced if these resources are already in place. The proposed methodology provides electric utilities with an energy-management tool to optimally utilize these resources and the storage systems to meet the HVAC load of the residential feeders at a desired confidence level.

Table 3: Ga Parameters.

Parameter	Population Size	Max Generation	Crossover Rate	Mutation Rate	Elitism Number
Value	200	150	78%	20%	2

Table 4: Simulation Results For Ga-Based and Classical Optimization Approaches.

Simulation Results	$\alpha_w(MW)$	$\alpha_{pv}(MW)$	$S(MWh)$	$EE(MWh)$	Total Cost (M\$)
GA (MATLAB)	1.9325	0	3.383	1.148	4.7792
DNLP (GAMS)	1.9350	0	3.392	1.171	4.786

Case Studies I and II show the economic benefits of using wind power to supply the HVAC load. This is evident from the lower installation costs of the hybrid system in Case Study I with respect to Case Study II. In addition, optimal solutions for Case Study I require less wind power capacity than the PV power capacity of Case Study II. The simulation results summarized in Table II provide a quantitative representation of the compromise between cost and risk in the hybrid system.

IV. CONCLUSION

This paper evaluates the efficiency of a hybrid system that combines renewable energy generation and energy storage to meet a controllable HVAC load. Using historical data and curve fitting, wind and PV generation and cooling loads are stochastically modeled. FCM clustering provides ten data clusters that properly represent the effects of seasonal variations. GA-based optimization is proposed to minimize the cost and increase the efficiency. A smart-grid strategy is developed to shift the load and match the renewable energy generation and cooling load. This method is tested on a residential feeder and different case studies are carried out to investigate the factors affecting the energy efficiency of the system. The proposed procedure can be applied for any controllable deferrable load, such as the HVAC load. Simulation results show that increasing the LS percentage gives the system more flexibility and may lead to less excess energy and more efficiency. Our results show the compromise between the risk of failure to meet demand and cost for different wind and PV generation levels. Case studies demonstrate the economic benefits of using wind power to supply the HVAC load. In addition, the proposed methodology provides utility companies with an energy-management tool to optimally utilize the installed renewable energy sources and the storage system to meet the flexible loads of the residential/commercial/industrial feeders. For future work, we will apply the proposed method to matching the renewable energy sources with other controllable loads, such as plug-in electric vehicles.

REFERENCES

- [1] [Online]. Available: <http://www.ita.ucla.edu/news/presentations/Ton-UCLA1119-rv.pdf> System Operator, CAISO report, Nov. 2007.
- [2] C. Loutan and D. Hawkins, Integration of renewable resources: Transmission and operating issues and recommendations for integrating renewable resources on the California ISO-controlled grid California Independent System Operator, CAISO report, Nov. 2007.
- [3] T. Ackermann, *Wind Power in Power Systems*. Hoboken, NJ: Wiley, 2005.
- [5] Began and R. Billinton, "Evaluation of different operation strategies in small stand-alone power systems," *IEEE Trans. Energy Convers.*, vol. **20**, no. 3, pp. 654–660, Sep. 2005.
- [6] D. B. Nelson, M. H. Nehrir, and C. Wang, "Unit sizing of stand-alone hybrid wind/PV/fuel cell power generation systems," in *Proc. IEEE Power Eng. Soc. Gen. Meeting*, 2005, pp. 2115–2122.
- [7] B. S. Borowy and Z. M. Salameh, "Methodology for optimally sizing the combination of a battery bank and PV array in a wind/PV hybrid system," *IEEE Trans. Energy Convers.*, vol. **11**, no. 2, pp. 367–375, Jun. 1996.
- [8] O. C. Onar, M. Uzunoglu, and M. S. Alam, "Modeling, control and simulation for an autonomous wind turbine/photovoltaic/fuel cell/ultra-capacitor hybrid power system," *J. Power Sources*, vol. **185**, no. 2, pp. 1273–1283, Dec. 2008.
- [9] C. Wang and M. H. Nehrir, "Power management of a stand-alone wind/ photovoltaic/fuel cell energy system," *IEEE Trans. Energy Convers.*, vol. **23**, no. 3, pp. 957–967, Sep. 2008.
- [10] S. R. Connors, J. G. McGowan, and J. F. Manwell, "Wind/diesel village-scale electric power systems: The performance and economic analysis of a simulated village system," *Solar Wind Technol.*, vol. **7**, no. 4, pp. 423–439, 1990.
- [11] F. Bonanno, A. Consoli, S. Lombardo, and A. Raciiti, "A logistical model for performance evaluations of hybrid generation systems," *IEEE Trans. Ind. Appl.*, vol. **34**, no. 6, pp. 1397–1403, Dec. 1998.
- [12] C. Abbey, J. Robinson, and G. Joos, "Integrating renewable energy sources and storage into isolated diesel generator supplied electric power systems," presented at the 13th Conf. Power Electron. Motion Control, Poznan, Poland, Sep. 2008.
- [13] E. I. Vrettos and S. A. Papathanassiou, "Operating policy and optimal sizing of a high penetration RES-BESS system for small isolated grids," *IEEE Trans. Energy Convers.*, vol. **26**, no. 3, pp. 744–756, Sep. 2011.
- [14] T. Senjyu, D. Hayashi, A. Yona, N. Urasaki, and T. Fumabashi, "Optimal configuration of power generating systems in isolated island with renewable energy," *Renew. Energy*, vol. **32**, no. 11, pp. 1917–1033, Sept. 2007.
- [15] R. Dufo-Lopez and J. L. Bernal-Agustin, "Multi-objective design of PV-wind-diesel-hydrogen-battery system," *Renew. Energy*, vol. **33**, no. 12, pp. 2559–2572, Dec. 2008.
- [16] R. Chedid and S. Rahman, "Unit sizing and control of hybrid wind solar power systems," *IEEE Trans. Energy Convers.*, vol. **12**, no. 1, pp. 79–85, Mar. 1997.
- [17] L. Wang and C. Singh, "Multicriteria design of hybrid power generation systems based on a modified particle swarm optimization algorithm," *IEEE Trans. Energy Convers.*, vol. **24**, no. 1, pp. 163–172, Mar. 2009.
- [18] S. Diaf, D. Diaf, M. Belhamel, M. Haddadi, and A. Louche, "A methodology for optimal sizing of autonomous hybrid PV/wind system," *Energy Policy*, vol. **35**, pp. 5708–5718, Aug. 2007.
- [19] G. Tina, S. Gagliano, and S. Raiti, "Hybrid solar/wind power system probabilistic modeling for long-term performance assessment," *Solar Energy*, vol. **80**, pp. 578–588, Jun. 2005.
- [20] K. Zou, A. P. Agalgaonkar, K. M. Muttaqi, and S. Perera, "Distributionsystem planning with incorporating DG reactive capability and system uncertainties," *IEEE Trans. Sustain. Energy*, vol. **3**, no. 1, pp. 112–123, Jan. 2012.
- [21] J. C. Bezdek, *Pattern Recognition With Fuzzy Objective Function Algorithms*. New York: Plenum, 1981.
- [22] [Online].
- [23] D. J. Ketchen and C. L. Shook, "The application of cluster analysis in strategic management research: An analysis and critique," *Strat. Manage. J.*, vol. **17**, pp. 441–458, 1996.

- [24] S. Roy, "Market constrained optimal planning for wind energy conversion systems over multiple installation sites," *IEEE Trans. Energy Convers.*, vol. **17**, no. 1, pp. 124–129, Mar. 2002.
- [25] Y.M. Atwa, E. F. El-Saadany, M.M. A. Salama, R. Seethapathy, M. Assam, and S. Conti, "Adequacy evaluation of distribution system including wind/solar DG during different modes of operation," *IEEE Trans. Power Syst.*, vol. **26**, no. 4, pp. 1945–1952, Nov. 2011.
- [26] V. A. Graham and K. G. T. Hollands, "A method to generate synthetic hourly solar radiation globally," *Solar Energy*, vol. **44**, pp. 333–341, 1990.
- [27] [Online]. Available: <http://www.ecodirect.com/Solar-Power-Inverter-Comparison-s/247.htm>
- [28] [Online]. <http://www.greenworldinvestor.com/topics/solar-renewable-energy-greeninvest/solar-inverters/>
- [29] T. Weise, *Global Optimization Algorithms—Theory and Application*, 2nd ed. Hefei, China: Thomas Weise, Jun. 26, 2009. [Online]. <http://www.it-weise.de/projects/book.pdf>
- [30] Z. Xu, Z. Y. Dong, and K. P. Wong, "Transmission planning in a deregulated environment," *Proc. Inst. Elect. Eng., Gen. Transm. Distrib.*, vol. **153**, no. 3, May 2006.
- [31] P. Maghouli, S. H. Hosseini, M. O. Buygi, and M. Shahidehpour, "A multi-objective framework for transmission expansion planning in deregulated environments," *IEEE Trans. Power Syst.*, vol. **24**, no. 2, pp. 1051–1061, May 2009.
- [32] T. Mosher, "Economic valuation of energy storage coupled with photovoltaic: current technologies and future projections," M.Sc. dissertation, Dept. Aeronaut. Astronaut., Mass. Inst. Technol., Cambridge, MA, June 2010.
- [33] A. Schellenberg, W. Rosehart, and J. Aguado, "Cumulant-based probabilistic optimal power flow (p-opf) with gaussian and gamma distributions," *IEEE Trans. Power Syst.*, vol. **20**, no. 2, pp. 773–781, May 2005.
- [34] G. J. Hahn and S. S. Shapiro, *Statistical Models in Engineering*. New York: Wiley, 1967.
- [35] M. Madrigal, K. Ponnambalam, and V. H. Quintana, "Probabilistic optimal power flow," in *Proc. IEEE Can. Conf. Elect. Comput. Eng.*, May 1998, pp. 385–388.
- [36] W.D. Tian, D. Sutanto, Y. B. Lee, and H.R. Outhred, "Cumulant based probabilistic power system simulation using Laguerre polynomials," *IEEE Trans. Energy Convers.*, vol. **4**, no. 4, pp. 567–574, Dec. 1989.
- [37] E. Rosenblueth, "Point estimation for probability moments," *Proc. Nat. Acad. Sci. United States Amer.*, vol. **72**, no. 10, pp. 3812–3814, Oct. 1975.
- [38] C. Su and C. Lu, "Two-point estimate method for quantifying transfer capability uncertainty," *IEEE Trans. Power Syst.*, vol. **20**, no. 2, pp. 573–579, May 2005.
- [39] G. Verbic and C. A. Canizares, "Probabilistic optimal power flow in electricity markets based on two-point estimate method," *IEEE Trans. Power Syst.*, vol. **21**, no. 4, pp. 1883–1893, Nov. 2006.
- [40] [Online]. <http://transmission.bpa.gov/business/operations/wind/>
- [41] [Online]. http://www.nrel.gov/eis/pdfs/uwig_spring_2011_speckman.pdf
- [42] Alternative sectoral load shapes for NEMS, Aug. 2001.
- [43] G. Barbose, N. Darghouth, R. Wiser, and J. Seel, *Tracking the Sun*
- [44] R. Wiser and M. Bolinger, U.S. Dept. Energy, "2010 Wind Technologies Market Report," Jun. 2011.